Environmental Science
Water Research & Technology

ROYAL SOCIETY OF CHEMISTRY

PAPER

View Article Online
View Journal

Cite this: DOI: 10.1039/d6ew00148c

Chlorination and bromination of nucleobases: the role of cytosine and adenine in the formation of disinfection byproducts

Julia E. Stroud, Kumudu H. Rathnayake and Susana Y. Kimura *

Received 9th February 2026,
Accepted 11th May 2026

DOI: 10.1039/d6ew00148c

rsc.li/es-water

Freshwater sustainability is increasingly challenged by population growth, climate change, and rising economic demands—prompting greater reliance on alternative water sources such as recycled wastewater. Water disinfection is used to inactivate pathogens but can also unintentionally generate disinfection byproducts (DBPs), which pose significant health risks with long-term exposure. Wastewater contains elevated levels of ammonia and organic nitrogen sources—such as nucleobases—promoting the formation of toxic unregulated nitrogen-containing DBPs (N-DBPs). Chlorine (HOCl) and *in situ* disinfectants like bromine (HOBr) can react with nitrogenous compounds to produce *N*-halamines which may serve as precursors to N-DBPs. The present work investigated the formation and stability of *N*-halamines from reactions between chlorine or bromine and two nitrogen-rich model compounds (cytosine and adenine) under varying pH and stoichiometric ratios. Using ultraviolet-visible (UV-vis) spectrophotometry and tandem mass spectrometry, it was elucidated that the reaction between chlorine with both adenine or cytosine produced mono- and possibly di-substituted *N*-chloramines, whereas reactions with bromine produced carbon-substituted brominated final products. DBP formation potential experiments showed that chlorinated and brominated nucleobases continued to react with organic matter (humic acid) to produce both C- and N-DBPs at moderate concentrations similar to monochloramine. This work provides insight into the role of *N*-halamines and brominated nitrogenous compounds in the production of N-DBPs and should inform future policy working towards further regulating N-DBPs in our potable water.

Water impact

Recycled wastewater is increasingly contributing to drinking water supplies through both planned and unintentional reuse, but chemical disinfectants may react with organic nitrogen sources—like nucleobases—and promote unregulated nitrogen-containing DBPs (N-DBPs). *N*-chloramines and C-brominated nucleobases were formed from the reaction of chlorine or bromine with nucleobases; however, when reacted with organic matter, only moderate DBP concentrations resulted—contributing to N-DBP regulation efforts.

1. Introduction

The sustainability of freshwater supplies is of growing concern due to population growth, uncertain climate patterns, and increasing economic demands. As a result, there is increased reliance on alternative water sources, including the reuse of wastewater effluents, which contain various contaminants such as pathogens,[1] halide ions,[2] pesticides,[3] pharmaceuticals,[4] and personal care products.[5] Thus, the reuse of wastewater requires disinfection practices to mitigate outbreaks of waterborne diseases. Chlorine-based disinfectants are commonly used in water disinfection; however, they may unintentionally form disinfection by products (DBPs) which can cause unfavourable health effects through chronic exposure, such as bladder cancer and adverse birth outcomes.[6–14] Moreover, wastewater effluents contain high levels of ammonia and organic nitrogen (primarily in the form of amino acids, peptides, and nucleic acids) that may lead to the formation of unregulated nitrogenous-DBPs (N-DBPs). This is of concern because N-DBPs have been observed to be more cytotoxic than currently regulated carbonaceous DBPs (C-DBPs) despite lower reported concentrations.[15–18] Some of the most toxic DBPs are those containing halogens being, in decreasing order of reported toxicity: iodinated, brominated, and chlorinated DBPs.[19–21]

Department of Chemistry, University of Calgary, 2500 University Dr. NW, Calgary, AB T2N 1N4, Canada. E-mail: s.kimurahara@ucalgary.ca

Chlorine (HOCl) reacts with bromide (Br^-) to form hypobromous acid (HOBr), a potent secondary chemical disinfectant.[21–23] Both hypohalous acids rapidly react with nitrogen-containing compounds in wastewater effluents to produce *N*-halamines, possible key precursors to N-DBPs.[24–27] Given the persistence of eukaryotic, prokaryotic, and viral genetic material in wastewaters,[28,29] adenine and cytosine—a purine and pyrimidine, respectively, which are building blocks of both DNA and RNA—were selected to investigate *N*-halamine and N- and C-DBP formation potential. These two nucleobases were selected over the other three (guanine, thymine, and uracil) because they provide complimentary functionalities of the two types of bases such that the influence of base structure on *N*-halamine formation and DBP pathways could be assessed and compared. Moreover, while cytosine is suggested to produce the most DBPs of all the nucleobases[30] (making it an appropriate 'model' pyrimidine), adenine's stability confers a higher likelihood of stable *N*-halamine formation from halogenation than guanine (which is slightly more reactive due to its C6 carbonyl). Purines and pyrimidines have been identified in occurrence studies at concentrations in the range of μg L^{-1}—with adenine being reported at concentrations of 3.7 μg L^{-1} in drinking water supplies.[31–33]

The chlorination of these nucleobases has been examined previously. By employing electrospray ionization (ESI)-tandem mass spectrometry (MS/MS),[31] Xiang *et al.* demonstrated that chlorination can occur at both the heterocyclic ring and the exocyclic aliphatic amine groups of adenine and cytosine; their study observed distinct pH-dependent transformations, such as the formation of an 8-chloro derivative of adenine at pH 4, but not at pH 7, and the identification of 5-chlorocytosine and 4-*N*-chlorocytosine as cytosine transformation products.[30] Complementary work by Zhang *et al.*[22,34] showed that chlorination of adenine and cytosine generates a variety of N-DBPs arising primarily from 3-monochlorocytosine, 5-monochlorocytosine, and 3,5-dichlorocytosine—emphasizing the involvement of *N*-halamine intermediates in DBP formation through UV/chlorine treatment processes. In a more recent study, Sun *et al.* (2023)[35] identified several halogenated nucleobases, including 2-chloroadenine, 6-chloroguanine, and 5-bromouracil, as emerging DBPs in drinking water—with concentrations up to 65.3 ng L^{-1}. Notably, 2-chloroadenine exhibited significant cytotoxicity, re-iterating the health risks associated with nucleobase-derived byproducts.[35]

Despite these findings, the specific conditions favoring the formation of stable *N*-halamines from adenine and cytosine, and their subsequent potential to produce DBPs relative to known disinfectants, remains unclear. Furthermore, previous studies have not identified *N*-halamines particularly because they used quenchers that would destroy them.[22,31,34,35] Additionally, a knowledge gap exists in understanding the specific conditions under which halogenation of environmental free nucleobases occurs; although, some studies discuss nucleoside bromination with bromine addition primarily occurring on the C5 position of cytosine.[36,37] As such, the stability and occurrence of resulting *N*-bromamines, as well as their potential to form DBPs in the presence of organic matter appears to not be well understood. Addressing these gaps is crucial for assessing the safety of water treatment processes and mitigating the formation of harmful byproducts. The work described herein aims to (1) determine under which conditions the chlorination and bromination of cytosine and adenine generate stable *N*-halamines using UV-visible (UV-vis) spectrophotometry and MS/MS, and (2) evaluate the DBP formation potential of the produced *N*-halamines with Humic Acid. This study should contribute to policy or efforts to mitigate N-DBP formation during wastewater defacto and potable re-use for drinking water purposes.

2. Materials and methods

2.1 Chemicals and reagents

Cytosine (≥99%), adenine (99%), sodium phosphate monobasic (≥98%), sodium bicarbonate (99.7%), sodium acetate(98%), sodium bromide (≥99%), sodium sulfite (≥98.0%), sodium hydroxide (98.0%), potassium iodide (≥99%), reagent-grade NaOCl, *N*-*N*-diethyl-*p*-phenyl-enediamine sulfate salt (DPD, ≥98.0%), ammonium chloride (≥99.5%), 1,3,5-trimethoxybenzene (TMB, ≥99%), nitrobenzene (≥99.0%), 2-bromo-1,3,5-trimethoxybenzene (Br-TMB, $C_9H_{11}BrO_3$; ≥99.9%) toluene (≥99.9%), and 37% hydrochloric acid were sourced from Sigma-Aldrich (St. Louis, MO, USA). 5-Bromocytosine (>98.0%) was sourced from TCI America (Portland, OR, USA). LC-MS/MS grade methanol, anhydrous acetonitrile (ACN), and water as well as methyl *tert*-butyl ether (MTBE, 99.9%) were acquired from Fisher Scientific (New Hampshire, USA).

Purity and vendor information for reference standards for 25 DBPs representing six DBP families: trihalomethanes, haloacetonitriles, haloketones, halonitromethanes, haloacetaldehydes, and iodo-trihalomethanes are shown in Table S1 in the (SI).[38] Suwanee River humic acid (SRHA) was purchased from the International Humic Substances Society (St. Paul, MN, USA).

Ultrapure water used in this study was distilled, deionized, and subjected to ultra-purification through a Barnstead B-Pure system, followed by a Barnstead MicroPure UV/UF system. Produced water (resistivity ≥18.2 MΩ cm^{-1}, organic carbon content <5 ppb) was used to prepare chlorine demand free water following Standard Method 4500-Cl C (ref. 39) as well as chlorine demand free glassware, based on external established methods.[40] DBP reference standard solutions were prepared as described by Ortega *et al.* (2021) (Text S1 in the SI).[41]

HOBr was prepared according to previously published methods from sodium hypochlorite and sodium bromide over three days and standardized before use *via* UV-vis spectrophotometry (model UV-2700, Shimadzu Corp., Japan) at a wavelength of 329 nm (molar absorptivity = 332 M^{-1} cm^{-1}).[42,43] NH_2Cl was prepared as described elsewhere by mixing NaOCl and NH_4Cl in a 1 to 1.1 molar ratio at a

controlled pH of 8.0 to minimize dichloramine formation.[44,45] NH_2Cl was standardized at a wavelength 243 nm (molar absorptivity = 461 M^{-1} cm^{-1}).[46]

2.2 Chlorination/bromination of cytosine and adenine

All reaction samples were prepared with chlorine demand free water. The reagent-grade NaOCl stock solution was standardized before use with UV-vis spectrophotometry at a wavelength of 292 nm (molar absorptivity = 350 M^{-1} cm^{-1}).[43,45] Cytosine and adenine chlorination/bromination reactions were conducted at pH 4.0 with a 5 mM acetate buffer, 7.0 with a 5 mM phosphate buffer, and 10.0 with a 5 mM carbonate buffer. Three Cl/P (chlorine-to-pyrimidine/purine) molar ratios (10 : 1, 1 : 1, and 0.1 : 1) were assessed at each pH condition. Experiments were conducted at pH 4.0, 7.0, and 10.0 to capture the effect of pH on free chlorine and bromine speciation (HOCl/HOBr *vs.* OCl^-/OBr^-) and reactivity to include both environmentally relevant (pH 7.0) and mechanistic (pH 4.0 and 10.0) extremes. Oxidant-to-pyrimidine/purine molar ratios (10 : 1, 1 : 1, 0.1 : 1) were selected to represent oxidant-excess, near-stoichiometric, and pyrimidine/purine-excess conditions to assess how *N*-halamine formation is affected by oxidant availability. All 36 reactions were maintained at 430 rpm in 125 mL Erlenmeyer flasks covered with aluminum foil to prevent light exposure, with a final reaction volume of 100 mL. For reaction monitoring by UV-vis, 3 mL aliquots were collected at 2, 5, 10, 20, and 30 min as well as at 1, 2, 3, 18, 24, 48, and 72 hours after chlorine/bromine addition, and immediately analyzed using a UV-vis spectrophotometer from 200–400 nm in 1 nm increments. Control experiments were also performed being either cytosine/adenine, or HOCl/HOBr in buffered water at specific pH conditions. Potential interference between the acetate buffer (at pH 4.0) and free chlorine was evaluated by monitoring the HOCl controls for pH 4.0 reactions at 0 and 20 hours later (Fig. S1A in the SI), which showed no measurable change in the absorbance over time as reported from other studies.[47] The free and combined chlorine residual throughout reactions was determined with the DPD colorimetric method.[39] Reaction aliquots (in triplicate) were collected at varying time points (0, 2, 5, 20, 30 min and 2, 18, 24, 48, 72 h) after chlorine/bromine addition.

Bromine and combined bromine (+1 oxidation state) were determined using TMB as a derivatization agent to produce Br-TMB as per published protocols.[48,49] Briefly, a 1 mL aliquot of each solution were transferred to glass centrifuge tubes (in triplicate) and reacted with 80 μM TMB at the same time-points as employed in the DPD method (0, 2, 5, 20, 30 min and 2, 18, 24, 48, 72 h). Then the sample was extracted using liquid–liquid extraction with 0.5 mL toluene, shaken using a Burrel wrist-action shaker (Pittsburgh, PA, USA) for 2 min, followed by a 5 min rest period. Following this, 250 μL of the top layer (toluene) was transferred to a 2 mL amber vial and spiked with 6 μM nitrobenzene (internal standard). The extracts were immediately analyzed with gas chromatography tandem mass spectrometry (GC-MS/MS) to determine Br-TMB concentrations.

2.3 Intermediate and product confirmation with tandem mass spectrometry

A liquid–liquid extraction method based on published protocols[50–52] was used to extract both halogenated cytosine and adenine products at 2 and 24 h for chlorine reactions (timing based on DPD results) and immediately as well as after 2 h after mixing for bromine reactions (depending on Br-TMB and DPD results). Briefly, to 100 mL of the reaction mixture covered in aluminum foil, 10 mL of MTBE and 10 g of sodium sulfate were added, shaken for 10 min, followed by a 5 min resting period. The MTBE layer was passed through a sodium sulfate column to remove remaining water and concentrated to 1 mL using a TurboVap® II (Biotage, Uppsala, Sweden) under a gentle nitrogen gas flow of 1.0 L min^{-1} in a water bath at 32 °C. Subsequently, 10 mL of acetonitrile (ACN) was added to solvent exchange and then the extract was concentrated again to 1 mL. Finally, the 1 mL ACN extract was diluted with 1 mL of LC-optima grade water and transferred to 2 mL amber vials for MS analysis.

An ACQUITY H-class system equipped with a liquid chromatograph coupled to a Xevo TQ-S micro triple quadrupole mass spectrometer fitted with a *Z*-spray (dual orthogonal sampling) interface (Waters Corp., Milford, MA, USA) was used for analysis. Both positive and negative electrospray ionization modes were tested to maximize the ionization efficiency of molecular ions of pure cytosine and adenine prepared in a 1 : 1 ACN/water solution at concentrations of 5 ppm. The MS operation parameters used based on peak intensity *versus* background noise were ES+ mode, capillary voltage of 2.90 kV, a cone voltage of 15 V, an infusion flow rate of 5.0 μL min^{-1}, ion source temperature of 110 °C, desolvation temperature of 350 °C, desolvation gas flow rate of 600 L h^{-1}, and a cone gas flow rate of 50 L h^{-1}. To identify brominated products in reactions, reaction extract and standard (5-bromocytosine) were directly infused into a Thermoscientific (Waltham, MA USA) TSQ Fortis triple quadrupole mass spectrometer with an ESI probe (parameters: ES+ mode, ion spray voltage of 2.9 kV, an infusion flow rate of 5.0 μL min^{-1}, sheath gas at 4 L min^{-1}, sweep gas at 1.0 L min^{-1}, and ion transfer tube temperature at 350 °C) to monitor fragmentation with increasing collision energy. Fragmentation patterns were used to help identify brominated products.[38]

2.4 DBP formation potential experiments

Solutions in chlorine demand free water, covered in aluminum foil, were prepared consisting of 50 μM cytosine or adenine that were reacted first with 50 μM bromine or chlorine to form *N*-halamines (Br or Cl/P = 1). Then, 2 mg L^{-1} as C SRHA were added to solutions after 2 h (for chlorination experiments) or immediately after the reaction started (for bromination experiments). Control samples consisted of

cytosine or adenine with SRHA in buffered water. Combined chlorine formed from the reaction of chlorine with cytosine or adenine was quantified using the DPD method and reached a stable concentration after 2 h. This measured concentration was then used to set the doses of other oxidants (HOCl, HOBr, and NH_2Cl) added to SRHA. By matching oxidant concentrations, DBP formation potentials could be directly compared across the reaction mixture and the individual oxidants. Control, comparison, and reaction samples were made in headspace-free, 40 mL amber glass bottles. Samples were incubated at 25 °C for 1-, 2-, and 5-days and immediately extracted by liquid–liquid extraction in triplicate and analyzed with GC-MS/MS, according to a method described elsewhere.[41] Standard deviations for individual DBP concentrations, as well as standard deviations calculated from variances within DBP families, were determined and included in the DBP figures (raw data provided in the SI). Residual free and combined chlorine as well as free bromine were determined by the DPD colorimetric method[39] throughout these experiments.

DBPs were quantified with an Agilent 7890B with a multi-mode inlet coupled to a 7000C Agilent triple quadrupole (Agilent Technologies, Santa Clara, CA) with an electron ionization source. A previously developed multiple reaction monitoring method was used to quantify 6 DBP families (25 DBPs in total) including haloacetonitirles, halonitromethanes, haloacetaldehydes, iodo-trihalomethanes, trihalomethanes, and haloketones.[38,41] Optimized MS/MS conditions for all quantified DBPs are given in Table S1 in the SI. Further, calibration curves and solutions used for DBP quantification are detailed in Text 1 in the SI.

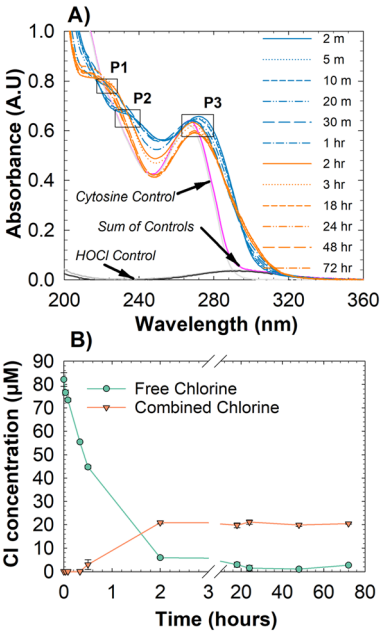

Fig. 1 (A) UV-vis spectra of the reaction between 0.1 mM cytosine and 0.1 mM free chlorine at pH 7.0 with 5 mM total phosphate buffer; (B) free and combined chlorine concentrations (n = 3) over time measured by the DPD method (0.1 mM cytosine, 0.1 mM NaOCl, 5 mM phosphate buffer). Error bars represent the standard deviation of the measured chlorine concentrations (n = 3). In (A), controls (HOCl control and cytosine control) were measured at t = 0 h and t = 20 h to ensure that there were no spectral changes over time. The sum of controls curve (pink) represents the spectra if no reaction occurred between reactants (determined from the sum of absorbance values of the individual controls). P1 = peak 1 at ~238 nm; P2 = peak 2 at ~226 nm, and P3 = peak 3 between ~275–280 nm.

3. Results and discussion

3.1 Chlorination of cytosine and adenine – *N*-chloramine formation assessment and confirmation

This study investigated reaction conditions which promote *N*-chloramine formation at three pH conditions (4.0, 7.0, 10.0) and three chlorine-to-pyrimidine/purine molar ratios (Cl/P = 0.1, 1, 10). Initial analyses were conducted at pH 7.0, as this condition is the most relevant in practice.[53] Reaction progress for the reaction of chlorine and cytosine with a molar ratio of 1 : 1 (Cl/Cyt = 1) at pH 7.0 was monitored by UV-vis spectrophotometry which revealed an isosbestic point around 295 nm, a transient peak appearing between 2–20 min at ~238 nm (P1), a transient peak between 2–3 hours at ~226 nm (P2), and a final peak (P3) with a blue shift between ~275–280 nm (Fig. 1A; S2A, B and Table S2 in SI). The isosbestic point is well established evidence of a single-step interconversion of reactants to product(s),[54] while the transient peaks point to short-lived intermediates or evolving reaction products. Previous studies have identified that nucleobase chlorination is associated with UV absorbance in the ~240–280 nm range—attributed to N–Cl bond formation.[55] Given that P3 had major maxima observed between ~275–280 nm which were both not observed in controls with cytosine or chlorine alone and were maintained over time (Fig. 1A), this provides possible evidence that a *N*-chloramine was formed and were maintained over time (Fig. 1A), this provides possible evidence that a *N*-chloramine was formed.

To further confirm whether the extra peaks or isosbestic point were due to *N*-chloramine formation, free and combined chlorine were quantified over time with the DPD method as shown in Fig. 1B (Table S3 in SI). Results suggest that combined chlorine (interpreted as *N*-chloramines) formation stabilized at ~2 h and persisted up to 72 h at an average concentration of 20.9 μM ± 0.5 μM (1.48 ± 0.04 mg L^{-1} as Cl_2)—a ~25% conversion from the initial free chlorine concentration (Fig. 1B), and consistent with reports that organic chloramines can be relatively persistent under water-treatment conditions.[56,57]

A reaction mixture sample was extracted at 2 h and directly infused into a mass spectrometer to confirm the formation of chlorinated species. The mass spectra (Fig. 2A) had two isotopic finger prints: one ion pair at ~146/148 m/z with a ~3 : 1 intensity ratio that indicates the presence of a monochlorinated species (and matches the m/z of cytosine plus one chlorine atom), and a second cluster at ~180/182/184 m/z with the expected ~9 : 6 : 1 intensity pattern that

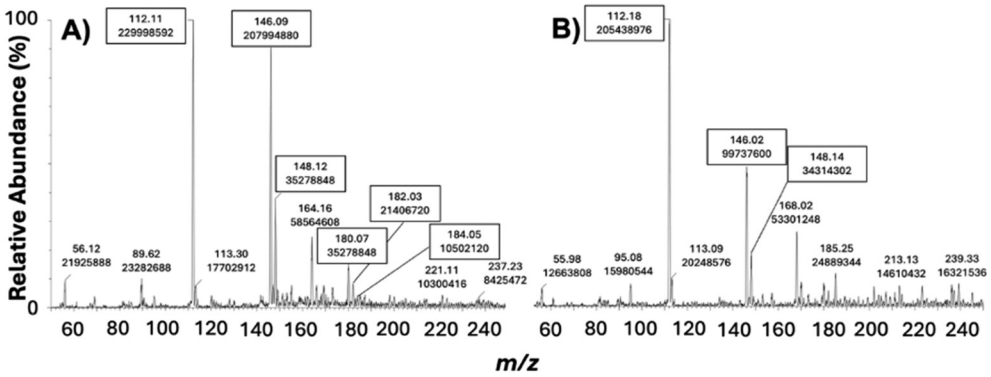

Fig. 2 MS1 spectra of direct injection (ESI+) of (A) a Cl/Cyt = 1, pH 7.0 reaction (50 mM cytosine, 50 mM NaOCl, 5 mM phosphate buffer) extracted after 2 hours of reaction initiation, and (B) Cl/Cyt = 1, pH 7.0 reaction extracted after 24 hours of reaction initiation. Peaks at ~112 *m*/*z* correspond to protonated cytosine; ~146 and 148 *m*/*z* at 3 : 1 intensity ratio correspond to mono-chlorinated cytosine; and ~180, 182, 184 *m*/*z* at 9 : 6 : 1 ratio correspond to di-chlorinated cytosine. Base peak intensity is 2.30×10^8 (A) and 2.05×10^8 (B). Collision energy = 0 eV.

indicates the presence of a dichlorinated species (and matches the *m*/*z* of cytosine and two chlorine atoms). Although, after 24 h, only the mono-chlorinated cytosine was observed at ~48% of the intensity compared to the 2 h sample (Fig. 2B). Together, the quantified combined chlorine concentration and the chlorinated cytosine isotope patterns at the *m*/*z* ratios expected support the assignment of mono- and di-chlorinated cytosine products in the 2 h extract under these reaction conditions, as well as the persistence of the mono-chlorinated nucleobase product in the 24 h extract—confirming the formation of stable *N*-chlorocytosine under these reaction conditions. However, due to the lack of analytical standards, confirmation of the exact structures of the mono- and di-chlorinated species was not possible.

There are three major sites in which halogenation of cytosine occurs: either i) on the exocyclic amine or ring nitrogens *via* generalized electrophilic attack or ii) on the ring carbons *via* electrophilic aromatic substitution (Fig. 3A–C). Electrophilic halogenation in water seems to be kinetically favored at exocyclic aliphatic and aromatic ring nitrogens (leading to *N*-halamine formation), whereas substitution at aromatic carbon sites seems to be thermodynamically favoured, proceeding through electrophilic aromatic substitution or rearrangement following intermediate *N*-halamine formation.[22,31,34] These general mechanisms could be applied to adenine chlorination as well as the bromination of both cytosine and adenine as discussed below. The reaction of chlorine and adenine with a molar ratio of 1 : 1 at pH 7.0 (Cl/Aden = 1) revealed a steady decrease in absorbance over time at ~210 and ~260 compared to controls (Fig. 4A; Fig. S2C, D and Table S4 in SI). Between 225–230 nm, fluctuations in intensity were observed in three clusters—with the 2–10 min absorbance increasing in intensity, the 20 min to 3 hours absorbance decreasing in intensity, followed by a decrease in absorbance over time from 18–72 hours (Fig. 4A). Combined chlorine formation appeared to stabilize around 2 h at a concentration of 5.29 μM ± 1.55 μM (0.38 ± 0.11 mg L^{-1} as Cl_2), a ~11% conversion from the initial free chlorine concentration and slowly declined to 4.72 μM ± 2.18 μM up to 72 h (Fig. 4B; Table S5 in SI). The observed lower reactivity is consistent with previous studies, as some observed only modest chlorine substitution for adenine (1–2 chlorines) compared to cytosine (1–4 chlorines), and noted that highly chlorinated adenine derivatives do not form at neutral pH under moderate Cl/P ratios.[31] Furthermore, MS experiments were carried out after 2 and 24 hours of reaction time; however, no chlorinated adenine clusters were observed at either time point, possibly due to low concentrations formed (data not shown). Results agree with Zhang *et al.* who showed faster degradation (and subsequent reactivity) for cytosine (first order rate constant $k = 6.49 \times 10^{-2}$

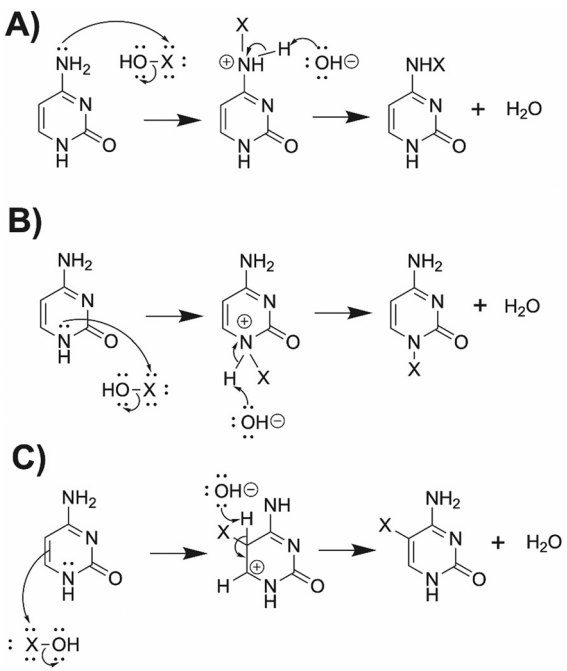

Fig. 3 Predominant mechanisms for halogenation of nucleobases at neutral pH—using cytosine halogenation (X = Cl or Br) as an example—with chlorination occurring at (A) aliphatic amines, (B) ring nitrogens, and (C) ring carbons on cytosine. Figure excludes resonance structures (only relevant resonance structure for reaction shown where applicable). Formation mechanisms supported by the literature.[22,30,33]

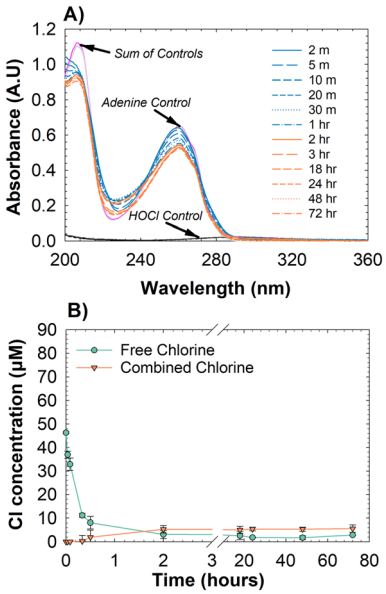

Fig. 4 (A) UV-vis spectra of reaction between 0.05 mM adenine and 0.05 mM free chlorine at pH 7.0 with 5 mM total phosphate buffer; (B) free and combined chlorine concentrations (n = 3) over time are shown (0.05 mM adenine, 0.05 mM NaOCl, 5 mM phosphate buffer).

min^{-1}) than for adenine (first order rate constant 4.13 × 10^{-2} min^{-1}) due to structural and electron availability differences between the two.[34] Adenine exhibits lower reactivity toward electrophilic halogenation than cytosine due to its larger, more extensively delocalized purine π-system (*i.e.*, due to its imidazole and purine rings systems), which distributes electron density and reduces the localization of reactive sites. In contrast, cytosine contains more defined regions of high electron density within its pyrimidine ring, particularly at C5 and N3, and a more localized electronic structure, making it more susceptible to electrophilic attack. Consequently, cytosine undergoes faster halogenation and degradation compared to adenine, consistent with previous observations that the reactive sites in cytosine (the C5–C6 double bond, ring nitrogens, and primary amine) are more susceptible to electrophilic attack than those in adenine's aromatic imidazole ring.[34] This also explains why there is a 5-fold higher concentration of *N*-chlorocytosine relative to *N*-chloroadenine (Fig. 1B and 4B). Moreover, no evidence of *N*-chloramine formation was observed in other Cl/P = 1 ratios at other pH conditions (pHs 4.0 and 10.0) for neither cytosine nor adenine (data not shown). The tested pH conditions influence both i) free halogen speciation (HOCl *vs.* OCl^-, $pK_a \approx 7.5$; HOBr *vs.* OBr^-, $pK_a \approx 8.8$) and ii) nucleobase protonation states, which together govern halogenation reactivity and product distribution. For example, in the case of chlorination at lower pH (pH 4.0), HOCl is the dominant species and is a strong electrophile; however, protonation of nucleobase functional groups can reduce nucleophilicity. At neutral pH (pH 7.0), a balance between reactive HOCl and unprotonated nucleophilic sites promotes efficient halogenation. At higher pH (pH 10.0), OCl^- predominates and exhibits lower electrophilicity, resulting in decreased reactivity.

Additionally, given that water disinfection practices often involve excess oxidant relative to nitrogenous precursors, reactions were also investigated at a ten-fold chlorine excess (Cl/P = 10). Under these conditions, the 10 : 1 reaction of chlorine and adenine (Cl/Aden = 10) at pH 4.0 displayed two transient peaks of two unknown compounds at ~220 and ~306 nm at the 5 min time-point (Fig. 5A; P1 and P2) that disappear by 1 h and 30 min, respectively (Fig. S2E–F and Table S6 in SI). Furthermore, the reaction reached an average combined chlorine concentration of 42.6 μM ± 3.2 μM ((3.02 ± 0.02) mg L^{-1} as Cl_2) between 2 to 72 h—a ~10% conversion from the initial free chlorine concentration (Fig. 5B; Table S7 in SI)—comparable in magnitude to that observed for the Cl/Aden = 1, pH 7.0 reaction. However, other excess-chlorine systems (Fig. S1B–F and Tables S8–S12 in SI) had negligible to no measurable *N*-chloramine formation. This outcome aligns with known behaviour of organic chloramines in that high oxidant doses often drive further oxidation or decomposition rather than stable *N*-chloramine accumulation.[58] The chlorine and cytosine reaction with a molar ratio of 10 : 1 (Cl/Cyt = 10) at pH 7.0 system depicts this concept well (Fig. S1B in SI), where the signal decreases gradually to almost 0 A.U. by the end of the experiment. Similarly, the low-oxidant dose reactions for both cytosine and adenine (Cl/P = 0.1) at all pH conditions tested (4.0, 7.0, 10.0) showed no measurable *N*-chloramine formation (data not shown); this is consistent with prior findings that sub-stoichiometric chlorine levels limit the formation of chlorinated-nucleobases and, instead, amine-chlorine complexes formed may revert to parent amines.[31,59]

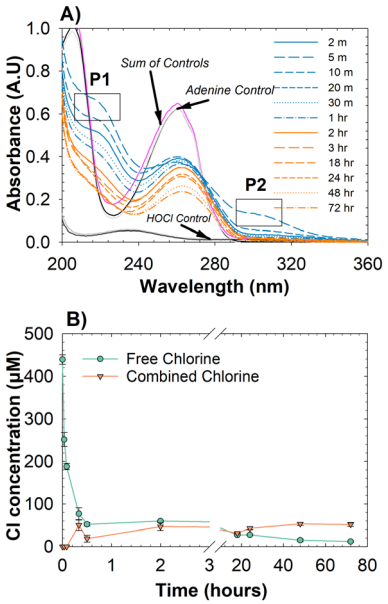

Fig. 5 For the reaction conditions Cl/Aden = 10, pH 4.0: (A) UV-vis spectra of reaction between 0.05 mM adenine and 0.5 mM free chlorine at pH 4.0 with 5 mM total acetate buffer; (B) free and combined chlorine concentrations (n = 3) over-time are shown (0.05 mM adenine, 0.5 mM NaOCl, 5 mM acetate buffer). P1 = peak 1 at ~220 nm. P2 = ~306 nm.

3.2 *N*-Chloramine DBP formation potential

N-Chloramine DBP formation potential was assessed for Cl/Cyt = 1 and Cl/Aden = 1 at pH 7.0 (Fig. 6A and B) by adding organic matter (SRHA) to the reaction mixtures after 2 h (time needed to form *N*-chlorocytosine and *N*-chloroadenine) and extracted after 1, 2, and 5 days. SRHA, the hydrophobic fraction of Suwanee River natural organic matter (SRNOM), was chosen because while both SRHA and SRNOM were identified as major DBP precursors,[60] SRHA was reported to be more reactive than SRNOM. *N*-Chlorocytosine reaction with SRHA (Fig. 6A; Table S13 in SI) produced a total DBP concentration of 6.63–9.07 μg L^{-1} across 5 d, primarily driven by trichloromethane with a maximum of 6.04 μg L^{-1}, followed by trichloroacetaldehyde (1.21–1.39 μg L^{-1}), dichloroacetonitrile (0.60–0.83 μg L^{-1}) and 1,1-dichloropropanone (0.31–0.38 μg L^{-1}), bromodichloromethane (0.24–0.26 μg L^{-1}), 1,1,1-trichloropropanone (0.037–0.15 μg L^{-1}), and tribromomethane (0.02–0.04 μg L^{-1}). Trichloromethane, trichloroacetaldehyde, bromodichloromethane, and tribromomethane were also observed in controls (cytosine and SRHA extracts; Fig. 6A and S3A in SI) but at lower concentrations (2.6, 0.58, 0.15, and 0.084 μg L^{-1}, respectively). Free chlorine in the *N*-chlorocytosine reaction mixture predominated after 1 d, while combined chlorine decreased from ~0.8 mg L^{-1} as Cl_2 after 1 d to between 0.0–0.2 mg L^{-1} as Cl_2 (Fig. S3B and Table S14 in SI).

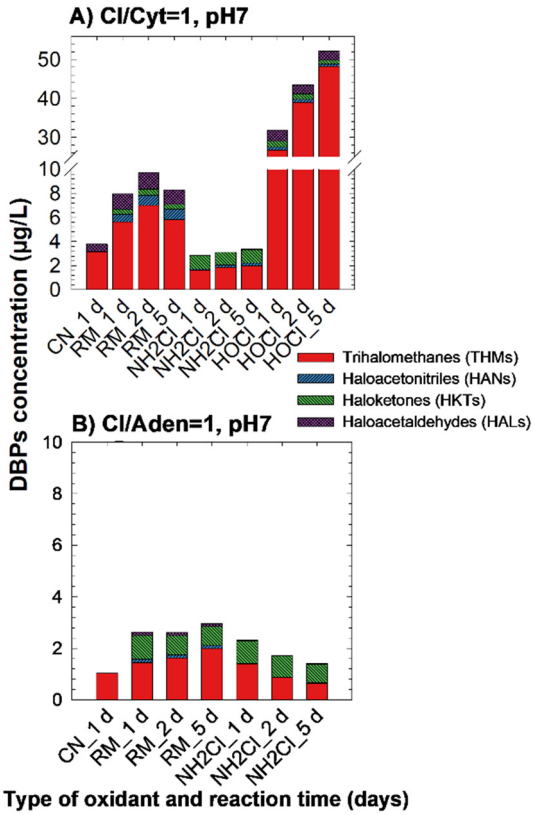

Fig. 6 Total DBPs shown by chemical family produced by (A) *N*-chlorocytosine formed under the reaction conditions: Cl/Cyt = 1, pH 7.0 (50 μM cytosine, 50 μM NaOCl, 5 mM phosphate buffer) and the (B) *N*-chloroadenine formed under the reaction conditions: Cl/Aden = 1, pH 7.0 (50 μM adenine, 50 μM NaOCl, 5 mM phosphate buffer). 'CN' refers to the control solution consisting of 50 μM cytosine or adenine + SRHA 2 mg L^{-1} as C; 'RM' corresponds to the reaction mixture consisting of 50 μM cytosine or adenine + 50 μM NaOCl + 2 mg L^{-1} as C SRHA; 'NH_2Cl' corresponds to the monochloramine comparison reaction solution consisting of 0.019 mM (A) or 0.0067 mM (B) NH_2Cl + 2 mg L^{-1} as C SRHA; 'HOCl' corresponds to the chlorine comparison reaction solution consisting of 0.019 mM (A) HOCl + 2 mg L^{-1} as C SRHA.

These results are consistent with literature findings that the chlorination of organic nitrogen precursors (*e.g.*, amino acids and amines) can promote the formation of both carbon- and nitrogen-based DBPs. While trihalomethanes are predominantly formed *via* the haloform reaction of activated carbonyl precursors, haloketones and haloacetaldehydes are produced from halogenation/oxidation of β-dicarbonyls and alcohol/aldehyde moieties, and haloacetonitriles formed through halogenation and oxidation of nitrogen-containing precursors such as amino acids and proteins.[61,62] *N*-Chlorocytosine DBP formation potential was compared with that of NH_2Cl and HOCl (Fig. 6A, S3C and D in SI, respectively). Trichloromethane was quantified in the largest amounts (1.6–2.0 μg L^{-1}) by NH_2Cl over 5 d; however, the control contained slightly higher trichloromethane levels (2.60 μg L^{-1}). NH_2Cl also produced other DBPs not found in the control, including, 1,1-dichloropropanone (0.99–1.0 μg L^{-1}), dichloroacetonitrile (0.11–0.27 μg L^{-1}), and 1,3-dichloropropanone (13DCP; 0.035–0.13 μg L^{-1}). Bromodichloromethane (0–0.039 μg L^{-1}) and trichloroacetaldehyde (0–0.025 μg L^{-1}) were also produced by NH_2Cl at lower concentrations compared to the control. Overall, NH_2Cl and *N*-chlorocytosine produced DBPs at comparable levels and within the same order of magnitude. While *N*-chlorocytosine yielded slightly higher concentrations of select C-DBPs (trihalomethanes and trichloracetaldehyde) and N-DBPs (dichloroacetonitrile), and lower haloketones relative to NH_2Cl, the overall distribution between C-DBPs and N-DBPs remained broadly similar. This suggests that the nucleobase-derived halamine does not fundamentally alter the suite of DBPs formed compared to inorganic chloramine. As expected, free chlorine was depleted by day 1 while combined chlorine increased to ~1.2–1.4 mg L^{-1} as Cl_2 after 1 d and remained constant (Fig. S3C and Table S15 in SI). In contrast, HOCl produced the highest total DBP levels of 32.7 μg L^{-1} at day 1, that increased up to 49.83 μg L^{-1} at day 5, primarily driven by trichloromethane (25.7–43.7 μg L^{-1}), followed by trichloroacetaldehyde (2.23–2.92 μg L^{-1}), bromodichloromethane (1.06–1.57 μg L^{-1}), 1,1,1-trichloropropanone (0.51–1.0 μg L^{-1}), dichloroacetonitrile (0.66–0.79 μg L^{-1}), tribromomethane (0.55–0.61 μg L^{-1}), 1,1-dichloropropanone (0.44–0.47 μg L^{-1}), and 1,1,3,3-tetrachloropropanone (0.05–0.20 μg L^{-1}). The free and combined chlorine concentrations in HOCl remained low after 1 d (Fig. S3D and Table S16 in SI). Results from this study align with the well-established notion that HOCl reactions with NOM favor trihalomethanes as dominant DBPs, whereas NH_2Cl generally produces lower DBP concentrations overall.[63–66]

In contrast to *N*-chlorocytosine, *N*-chloroadenine generated lower total DBP concentrations (2.68–3.03 μg L^{-1}) (Fig. 6B; Table S17 in SI), possibly due to the lower adenine reactivity as discussed above. At 1 d, trichloromethane was the highest DBP

quantified for *N*-chloroadenine (1.43 μg L^{-1}) which then increased up to 1.99 μg L^{-1} by 5 d. However, adenine controls (Fig. 6B and S4A in SI) produced a similar trichloromethane concentration (1.04 μg L^{-1}) indicating that trichloromethane was not significantly formed by *N*-chloroadenine. Haloketones were the second most predominant DBP family driven by 1,3-dichloropropanone, quantified up to 0.82 μg L^{-1} and decreased to 0.71 μg L^{-1} after 5 d. Other DBPs formed by *N*-chloroadenine that were negligible in controls include dichloroacetontrile and trichloroacetaldehyde (0.11–0.14 μg L^{-1}), bromodichloromethane (0.067–0.086 μg L^{-1}), 1,3-dichloroprpanone (0.189–0.082 μg L^{-1}), and 1,1,1-trichloropropanone (0–0.025 μg L^{-1}). Free chlorine was depleted by 1 d while the combined chlorine concentration plateaued around a low concentration of ~0.25 mg L^{-1} as Cl_2 (Fig. S4B and Table S18 in SI) throughout the 5 d. Overall, *N*-chloroadenine produced DBP quantities similar to NH_2Cl (Fig. S4C and Table S19 in SI)—although *N*-chlorocytosine produced higher amounts of DBPs overall. This is consistent with the behaviour of a weaker oxidant and aligns with studies that reported lower reactivities of purine precursors compared to pyrimidines as previously discussed.[22] Additionally, Zhang *et al.* have reported that pyrimidines (specifically uracil and cytosine) produce more C- and N-DBPs than purines.[22] Thus, the results suggest that the *N*-chlorocytosine and *N*-chloroadenine act as mild oxidants, producing both C- and N-DBPs in quantities comparable to monochloramine.

It is important to note that the nucleobase concentrations used in this study (50 μM) are substantially higher than those typically observed in recycled water (ng L^{-1} to μg L^{-1} range) and the simple buffered system does not account for the presence of ammonium and NOM. While these concentrations were required to study reactions using spectroscopic and mass spectrometric methods, they may not reflect environmentally relevant conditions. Furthermore, in practice, ammonium rapidly reacts with free chlorine to form inorganic chloramines, which are less reactive and can alter DBP formation. As a result, the reaction behavior and relative importance of nucleosides may differ under environmentally relevant conditions.

3.3 Bromination of cytosine and adenine – *N*-bromamine formation assessment

This study also evaluated *N*-bromamine formation from the reaction of HOBr with cytosine and adenine at three pH conditions (4.0, 7.0, 10.0) and three bromine-to-pyrimidine/purine molar ratios (Br/P = 0.1, 1, 10). Reaction progress for the reaction of bromine and cytosine with a 1 : 1 molar ratio (Br/Cyt = 1) at pH 7.0 revealed a transient peak appearing between 0–10 min at ~229 nm (P1 in Fig. 7A; Fig. S5A, B and Table S20 in SI) and the overall spectra seemingly depicts two different 'phases' of the reaction (*i.e.*, the blue traces appear distinct from the orange) suggesting short-lived product/intermediate formation. Lei *et al.* reported inorganic di- and mono-bromamines exhibit absorption maxima around 232 and 278 nm, respectively[42] which coincide with those

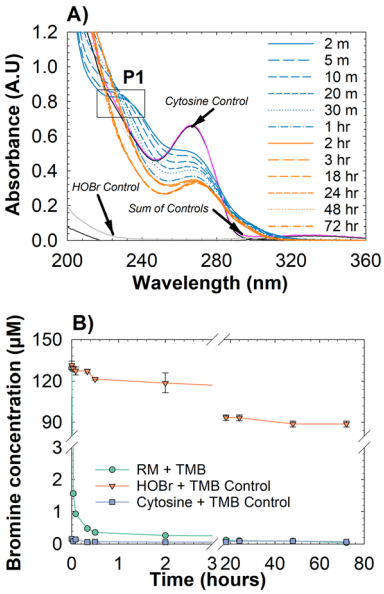

Fig. 7 (A) UV-vis spectra of reaction between 0.1 mM cytosine and 0.1 mM HOBr at pH 7.0 with 5 mM total phosphate buffer; (B) free and combined bromine measured in triplicate by Br-TMB signal in reaction mixture (RM) and control solutions. 'RM + TMB' is the brominated cytosine reacting with TMB over time (0.1 mM cytosine, 0.1 mM HOBr, 5 mM phosphate buffer). 'HOBr + TMB control' is a solution of bromine reacting with TMB over time (0.1 mM HOBr, 5 mM phosphate buffer). 'cytosine + TMB control' is cytosine reacting with TMB over time (0.1 mM cytosine, 5 mM phosphate buffer). Error bars represent the standard deviation of the sample.

observed in Fig. 7A. To further investigate whether bromine species were present, a derivatization method using GC-MS/MS (Br-TMB) was employed (Fig. 7B; Table S21 in SI). TMB was added to the HOBr and cytosine reaction mixture (green trace), where the bromine concentration rapidly declined and decreased to ~0 μM after ~2 h, suggesting that HOBr quickly reacted with cytosine and consumed all bromine oxidants in the +1-oxidation state (*e.g.* HOBr and *N*-bromamines) which was not observed in the HOBr control (Fig. 7B in orange). Previous studies have shown that under similar reaction conditions, carbon-substituted 5-bromocytosine forms by electrophilic aromatic substitution as a final product with an almost 90% predominance over other products.[36,37,67,68] Thus, although a transient peak P1 may indicate a short-lived *N*-bromamine, results seem to align with a carbon-substituted bromocytosine as the final reaction product—prompting further experimentation by MS.

Direct ES+ MS analysis of two sample extracts—one extracted just after the start of the reaction (~0 min) and another after 2 h—revealed evidence of a mono-brominated cytosine product with ion pairs at ~190/192 *m*/*z* with a 1 : 1 intensity ratio (Fig. 8) in both samples corresponding to the *m*/*z* of cytosine with one bromine atom. Results suggest that a stable bromocytosine is present after 2 h—most likely a carbon-substituted bromocytosine since *N*-bromamines are known to be unstable products.[69] To further corroborate this assignment, the fragmentation ions of precursor ion 190 *m*/*z*

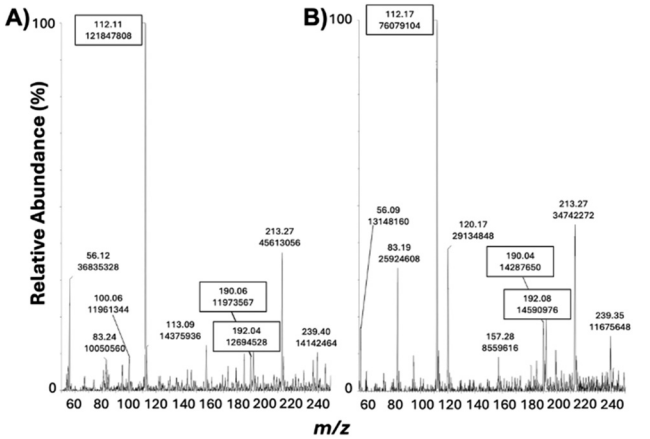

Fig. 8 MS1 spectra of the direct injection (ESI+) of a Br/Cy t= 1, pH 7.0 reaction (50 mM cytosine, 50 mM HOBr, 5 mM phosphate buffer) extracted (A) immediately after reaction initiation, and (B) Br/Cyt = 1, pH 7.0 reaction extracted after 2 hours of reaction initiation. Peaks at ~112 *m/z* correspond to protonated cytosine; ~190 and 192 *m/z* at a 1:1 intensity ratio correspond to mono-brominated cytosine. Base peak intensity is 1.22×10^8 (A), and 7.61×10^7 (B) collision energy = 0 eV.

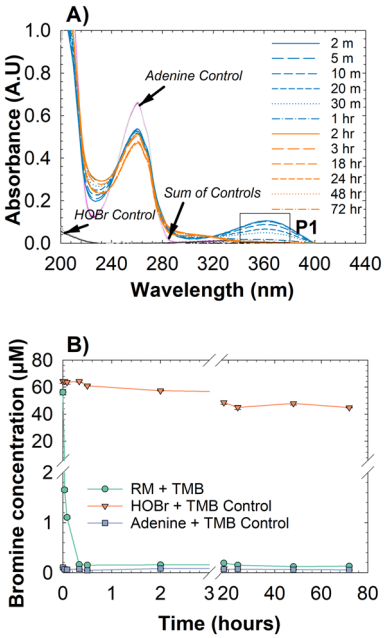

Fig. 9 (A) UV-vis spectra of reaction between 0.05 mM adenine and 0.05 mM HOBr at pH 7.0 with 5 mM total phosphate buffer; (B) free and combined bromine measured in triplicate by Br-TMB signal in reaction mixture (RM) and control solutions. 'RM + TMB' is the brominated adenine reacting with TMB over time (0.05 mM adenine, 0.05 mM HOBr, 5 mM phosphate buffer). 'HOBr + TMB control' is a solution of bromine reacting with TMB over time (0.05 mM HOBr, 5 mM phosphate buffer). 'Adenine + TMB control' is adenine reacting with TMB over time (0.05 mM adenine, 5 mM phosphate buffer).

were analyzed in a commercial 5-bromocytosine standard (Fig. S6A in SI) and compared to that of the reaction mixture extracted after 2 h of reaction progress (Fig. S6B in SI), showing that same fragmentation ions had similar abundance with the exception of 172/173 and 145/147 ions. In both cases, fragmentation was minimal below 15 eV, indicating that the precursor ion remains largely intact under low-energy conditions. Above 15–20 eV, the same product ions increase in relative abundance with increasing collision energy corresponding to expected loss of water and/or NH_3 (172/173 *m/z*, 1:1 intensity), secondary fragmentation while retaining bromine (145/147 *m/z*, 1:1 intensity), bromine loss (111 *m/z*), and possible cytosine ring fragments (possible other neutral losses; 84 *m/z*). As shown in previous studies, compounds exhibiting similar fragment ions but subtle differences in relative abundances over increasing collision energies are more consistent with structural isomers or mixtures of which rather than definitive confirmation of a single compound.[38] Thus, the differences observed on the relative abundances could indicate the presence of structural isomers (*e.g.*, 6-bromocytosine) or a mixture of both 5- and 6-bromocytosine.

For the reaction of bromine and adenine at pH 7.0, an isosbestic point at ~320 nm and a transient peak appearing between 0 min and 1 h at ~365 nm (P1 in Fig. 9A; Fig. S5C, D and Table S22 in SI) were observed. The transient peak suggests a short-lived product/intermediate that was formed and depleted within 1 h, and the isosbestic point suggests single-step product formation. MS experiments did not detect brominated species which contradicts with literature where *N*-bromamines and C-substituted bromoadenines were reported as products from the reaction of adenine analogs and bromine (*e.g.*, 8-bromoadenine) and absorb at less than 300 nm.[42,70–72] One possible explanation is that the transient peak at ~360 nm arises from short-lived intermediates, such as adeninyl radicals, aminyl species, or charge-transfer complexes, that absorb in this region, however this hypothesis requires further confirmation.[73,74] Furthermore, the total bromine concentration in the reaction mixture in Fig. 9B (green) (Table S23 in SI) was depleted by 20 min — which corroborates the fact that the formation of an active bromine species is unlikely.

Moreover, experiments conducted at other conditions (Br/P = 0.1 at pHs 4.0, 7.0, and 10.0; Br/P = 1 at pHs 4.0 and 10.0; and Br/P = 10 at pHs 4.0, 7.0, and 10.0) did not reveal the presence of *N*-bromamines. Previous studies have reported that in high-bromine concentration systems, direct oxidative halogenation dominates rather than stable halamine formation which might explain our results in reactions with Br/P = 10.[63]

3.4 Brominated nucleobase DBP formation potential

The bromocytosine and bromoadenine tentatively observed from the reaction of bromine and cytosine/adenine at pH 7.0 were assessed for DBP formation potential (Fig. 10A and B). With respect to the Br/Cyt = 1, pH 7.0 reaction (Fig. 10A; Table S24 and Fig. S7 in SI), bromocytosine produced a total DBP concentration of 7.51–10.07 μg L^{-1} primarily driven by tribromomethane (8.05–9.09 μg L^{-1}) and followed by dibromochloromethane (0.55–0.69 μg L^{-1}), bromodichloromethane (0.15–0.17 μg L^{-1}), dibromoacetonitrile (0.08–0.1 μg L^{-1}), and

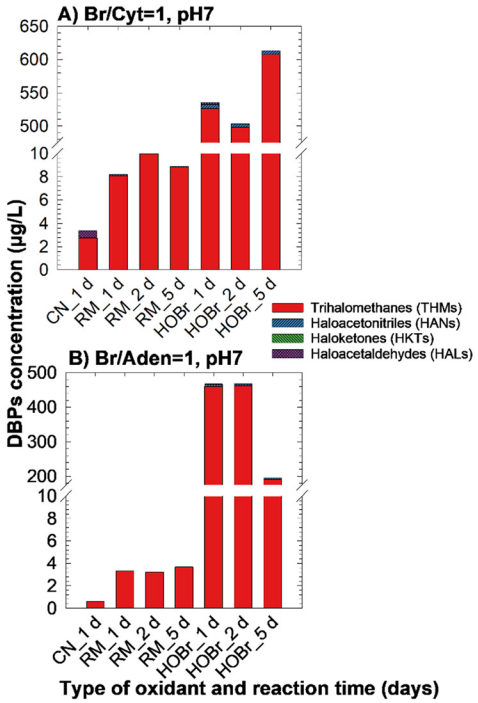

Fig. 10 Total DBPs shown by chemical family produced by the (A) bromocytosine formed under the reaction conditions: Br/Cyt = 1, pH 7.0 (50 μM cytosine, 50 μM HOBr, 5 mM phosphate buffer) and the (B) bromoadenine formed under the reaction conditions: Br/Aden = 1, pH 7.0 (50 μM adenine, 50 μM HOBr, 5 mM phosphate buffer). 'CN' refers to the control solution consisting of 50 μM cytosine or adenine + SRHA 2 mg L^{-1} as C; 'RM' corresponds to the reaction mixture consisting of 50 μM cytosine or adenine + 50 μM HOBr + 2 mg L^{-1} as C SRHA; 'HOBr' corresponds to the bromine comparison reaction solution consisting of 50 μM HOBr + 2 mg L^{-1} as C SRHA.

trichloromethane (0–0.041 μg L^{-1}) between 1 and 5 d. Also, the cytosine controls produced lower levels of total DBPs (~3.51 μg L^{-1}) including trichloromethane, trichloroacetaldehyde, bromodichloromethane, tribromomethane, and 1,1,1-trichloropropanone concentrations of 2.6, 0.58, 0.15, 0.11, and 0.026 μg L^{-1}, respectively—with trihalomethanes being the predominant DBP family (Fig. S7A in SI). In contrast, the HOBr reaction with SRHA produced a total DBP concentration of 470–580 μg L^{-1} over 5 d—about 50x more DBPs compared to bromocytosine. Primarily, tribromomethane was formed up to ~571 μg L^{-1} after 5 d, followed by dibromoacetonitrile (4.42–4.96 μg L^{-1}), dibromochloromethane (2.18–2.93 μg L^{-1}), tribromoacetaldehyde (0–2.73 μg L^{-1}), bromoacetontrile (0.90–0.94 μg L^{-1}), bromodichlormethane (0.19–0.23 μg L^{-1}), and trichloromethane (0–0.048 μg L^{-1}). DPD measurements show that the free bromine concentration plummeted by 24 h for both reactions (Fig. S7B-C and Table S25–26 in SI) which aligns with minimal DBP formation after this time point. Results suggest that after cytosine addition to HOBr, reactive halogen species (*N*-bromocytosine and possibly a small HOBr residual) reacted with SHRA to form the low DBP yields. DBP formation potential for the reaction mixture of bromine and cytosine with a molar ratio of 1 : 1 (Br/Cyt = 1) at pH 4.0 was also assessed due to the presence of isosbestic points observed during reaction progress monitoring and dibrominated cytosine observed in MS analysis (data not shown); however, *N*-bromamines were not observed and DBP formation was similar to that of the reaction at pH 7.0 only with reduced quantities—as is supported by the literature (Table S27 in SI).[38]

The reaction mixture of bromine and adenine with a 1 : 1 molar ratio (Br/Aden = 1) at pH 7.0 (Fig. 10B; Tables S28–S30, and Fig. S8 in SI) at 1 d produced a total DBP concentration of 3.16–3.52 μg L^{-1} primarily driven by tribromomethane (1.55–1.94 μg L^{-1}), with trace level concentrations of dibromochlormethane (0.8 μg L^{-1}), bromodichlormethane (0.49–0.50 μg L^{-1}), and trichloromethane (0.18–0.32 μg L^{-1}). In contrast, the HOBr reaction with SRHA generated up to ~500 μg L^{-1} TMB after 1 d followed by lower concentrations 0.38–4.56 μg L^{-1} of dibromoacetonitrile, dibromochloromethane, tribromoacetaldehyde, trichloromethane, bromodichlormethane, and bromoacetontrile. This showed that species from the bromine and adenine reaction produce significantly less DBPs compared to free bromine. Similar to the cytosine reaction, it is also possible that a small residual of free bromine could have reacted with SRHA to produce the observed DBPs instead. The main difference observed between the bromination of cytosine (Fig. 10A) and adenine (Fig. 10B) is that dibromoacetontrile (an N-DBP) was formed in the reaction of the brominated cytosine with SRHA.

4. Conclusions and future directions

In summary, the Cl/P = 1 and Br/P = 1 reactions at pH 7.0 showed spectral changes in reaction progress monitoring experiments which indicated product and/or intermediate formation. Further analysis suggested that *N*-chloramines may have been formed in chlorination reactions and C-brominated nucleobases being the primary final product(s) of the bromination reactions. Finally, DBP formation potential experiments showed that for Cl/P = 1, pH 7.0 reactions, *N*-chloramines produced both C- and N-DBPs at concentrations similar to monochloramine; for the Br/P = 1, pH 7.0 reactions, the cytosine reaction (Br/Cyt = 1, pH 7.0) produced both C- and N-DBPs while the adenine reaction (Br/Aden = 1, pH 7.0) only produced C-DBPs. Moreover, both the *N*-chloramines' and brominated nucleobases' DBP formation was primarily driven by trihalomethanes. Similarly, both bromination reaction conditions generally yielded DBPs at lower concentrations than free bromine; however, some DBPs (like bromodichloromethane) were produced at almost equal concentrations.

To the best of the authors' knowledge, previous studies have not investigated the bromination of cytosine and adenine within this context, and there exists a lack of identification of the conditions under which *N*-halamines form and remain stable enough to form DBPs. For example, studies that investigate the reaction of HOCl/HOBr with

nucleosides and nucleobases under similar conditions use quenchers (*e.g.*, ascorbic acid or sodium sulfite)[22,31,34,35] which, due to their strong reducing agent nature, can destroy any formed *N*-halamines. For that reason, in this study, the identification of stable *N*-halamines, the assessment of the bromination of nucleobases in general, and the investigation subsequent DBP formation from chlorinated and brominated intermediates establishes the current study as unique.

Due to the lack of commercially available standards for *N*-halamines, neither structure elucidation (halogenation occurring on exocyclic aliphatic nitrogens *versus* ring nitrogens) nor concrete mechanistic interpretation could be confidently proposed given the MS data. Future work should investigate nucleobase *N*-halamine formation in real world matrices, where increased chemical complexity and more realistic reactant concentrations can be considered. Additional work should also investigate the mechanisms by which DBPs were formed from the reaction products discussed herein to better inform regulatory and industry decision-making. Lastly, while SRHA was found to be more reactive, it may be useful to investigate DBP formation from other sources of organic matter and determine if they display higher reactivity toward *N*- or C-halonucleobases. Overall, this work contributes to the knowledge gap surrounding bromination (and chlorination, to an extent) of nucleobases, and their roles in C- and N-DBP formation—contributing to efforts to make wastewater disinfection practices safer.

Author contributions

JS carried out experimentation, data preparation and analysis, literature review, and wrote the manuscript. SYK reviewed and wrote the manuscript. KR carried out the GC-MS/MS DBP formation data analysis and contributed to the final version of the manuscript. All authors have read and approved the final version of the manuscript.

Conflicts of interest

There are no conflicts to declare.

Data availability

The data supporting this article have been included as part of the supplementary information (SI). SI includes a table of DBP parameters used for quantification; text of sample preparation for DBP quantification; figures of reactions between cytosine/adenine and HOCl/HOBr monitored with UV-vis, DBP formation potential by reaction intermediates, and relative abundances with increasing collision energy for 5-bromocytosine and reaction mixtures. Raw experimental data are also provided in the excel spreadsheet in SI.

Supplementary information is available. See DOI: https://doi.org/10.1039/d6ew00148c.

Acknowledgements

The authors would like to acknowledge Kyle Lee for initiating this study, as well as Dr. Tatek Temesgen Terfasa for troubleshooting advice. The methods used for GC-MS/MS analysis of DBP formation potential were developed by Jorge Alberto Perez Perez. Funding was provided by the Natural Sciences and Engineering Research Council (NSERC) Discovery Grant, Canada Research Chair, and Canada Foundation for Innovation.

References

1 A. M. Nasir, M. R. Adam, S. N. E. A. Mohamad Kamal, J. Jaafar, M. H. D. Othman, A. F. Ismail, F. Aziz, N. Yusof, M. R. Bilad, R. Mohamud, M. A. Rahman and W. N. Wan Salleh, A review of the potential of conventional and advanced membrane technology in the removal of pathogens from wastewater, *Sep. Purif. Technol.*, 2022, **286**, 120454, DOI: 10.1016/j.seppur.2022.120454.

2 J. E. Grebel, J. J. Pignatello and W. A. Mitch, Effect of halide ions and carbonates on organic contaminant degradation by hydroxyl radical-based advanced oxidation processes in saline waters, *Environ. Sci. Technol.*, 2010, **44**(17), 6822–6828, DOI: 10.1021/es1010225.

3 M. Köck-Schulmeyer, M. Villagrasa, M. López de Alda, R. Céspedes-Sánchez, F. Ventura and D. Barceló, Occurrence and behavior of pesticides in wastewater treatment plants and their environmental impact, *Sci. Total Environ.*, 2013, **458**, 466–476, DOI: 10.1016/j.scitotenv.2013.04.010.

4 A. M. Deegan, B. Shaik, K. Nolan, K. Urell, M. Oelgemöller, J. Tobin and A. Morrissey, Treatment options for wastewater effluents from pharmaceutical companies, *Int. J. Environ. Sci. Technol.*, 2011, **8**(3), 649–666, DOI: 10.1007/BF03326250.

5 M. Petrovic, Analysis and removal of emerging contaminants in wastewater and drinking water, *TrAC, Trends Anal. Chem.*, 2003, **22**(10), 685–696, DOI: 10.1016/S0165-9936(03)01105-1.

6 C. M. Villanueva, F. Fernández, N. Malats, J. O. Grimalt and M. Kogevinas, Meta-analysis of studies on individual consumption of chlorinated drinking water and bladder cancer, *J. Epidemiol. Community Health*, 2003, **57**(3), 166–173, DOI: 10.1136/jech.57.3.166.

7 C. M. Villanueva, K. P. Cantor, S. Cordier, J. J. Jaakkola, W. D. King, C. F. Lynch, S. Porru and M. Kogevinas, Disinfection byproducts and bladder cancer: a pooled analysis, *Epidemiology*, 2004, **15**(3), 357–367, DOI: 10.1097/01.ede.0000121380.02594.fc.

8 R. Grazuleviciene, V. Kapustinskiene, J. Vencloviene, J. Buinauskiene and M. J. Nieuwenhuijsen, Risk of congenital anomalies in relation to the uptake of trihalomethane from drinking water during pregnancy, *Occup. Environ. Med.*, 2013, **70**(4), 274–282, DOI: 10.1136/oemed-2012-101093.

9 M. J. Nieuwenhuijsen, P. Dadvand, J. Grellier, D. Martinez and M. Vrijheid, Environmental risk factors of pregnancy outcomes: a summary of recent meta-analyses of epidemiological studies, *Environ. Health*, 2013, **12**, 6, DOI: 10.1186/1476-069X-12-6.

10 K. Waller, S. H. Swan, G. DeLorenze and B. Hopkins, Female breast cancer and trihalomethane levels in drinking water in North Carolina, *Epidemiology*, 1998, **9**(2), 134–140, DOI: 10.1097/00001648-199803000-00006.

11 J. M. Wright, A. Evans, J. A. Kaufman, Z. Rivera-Núñez and M. G. Narotsky, Disinfection by-product exposures and the risk of specific cardiac birth defects, *Environ. Health Perspect.*, 2017, **125**(2), 269–277, DOI: 10.1289/EHP103.

12 S. W. Krasner, P. Westerhoff, B. Chen, B. E. Rittmann and G. Amy, Occurrence of disinfection byproducts in United States wastewater treatment plant effluents, *Environ. Sci. Technol.*, 2009, **43**(21), 8320–8325, DOI: 10.1021/es901611m.

13 M. Diana, M. Felipe-Sotelo and T. Bond, Disinfection byproducts potentially responsible for the association between chlorinated drinking water and bladder cancer: A review, *Water Res.*, 2019, **162**, 492–504, DOI: 10.1016/j.watres.2019.07.014.

14 S. D. Richardson, M. J. Plewa, E. D. Wagner, R. Schoeny and S. Demarini, Occurrence, genotoxicity, and carcinogenicity of regulated and emerging disinfection by-products in drinking water: a review and roadmap for research, *Mutat. Res., Rev. Mutat. Res.*, 2007, **636**(1–3), 178–242, DOI: 10.1016/j.mrrev.2007.09.001.

15 N. Liu, Z. Sun, H. Zhang, L. H. Klausen, M. Roh and S. Kang, Emerging high-ammonia-nitrogen wastewater remediation by biological treatment and photocatalysis techniques, *Sci. Total Environ.*, 2023, **875**, 162603, DOI: 10.1016/j.scitotenv.2023.162603.

16 T. Bond, J. Huang, M. R. Templeton and N. Graham, Occurrence and control of nitrogenous disinfection by-products in drinking water–a review, *Water Res.*, 2011, **45**(13), 4341–4354, DOI: 10.1016/j.watres.2011.05.034.

17 M. G. Muellner, E. D. Wagner, K. McCalla, S. D. Richardson, Y.-T. Woo and M. J. Plewa, Haloacetonitriles vs. regulated haloacetic acids: are nitrogen-containing DBPs more toxic?, *Environ. Sci. Technol.*, 2007, **41**(2), 645–651, DOI: 10.1021/es0617441.

18 T. K. Jayawardana, A. A. Goodarzi, E. U. Kurz, T. Temesgen and S. Y. Kimura, Toxicity of haloacetonitrile mixtures to a normal tissue-derived human cell line: are they additive, synergistic, or antagonistic?, *Environ. Sci. Technol. Lett.*, 2025, **12**(5), 476–481, DOI: 10.1021/acs.estlett.5c00200.

19 E. D. Wagner and M. J. Plewa, CHO cell cytotoxicity and genotoxicity analyses of disinfection by-products: An updated review, *J. Environ. Sci.*, 2017, **58**, 64–76, DOI: 10.1016/j.jes.2017.04.021.

20 M. R. Rose and A. L. Roberts, Iodination of dimethenamid in chloraminated water: Active iodinating agents and distinctions between chlorination, bromination, and iodination, *Environ. Sci. Technol.*, 2019, **53**(20), 11764–11773, DOI: 10.1021/acs.est.9b03645.

21 Y. Pan, X. Zhang, E. D. Wagner, J. Osiol and M. J. Plewa, Boiling of simulated tap water: effect on polar brominated disinfection byproducts, halogen speciation, and cytotoxicity, *Environ. Sci. Technol.*, 2014, **48**(1), 149–156, DOI: 10.1021/es403775v.

22 B. Zhang, Q. Xian, T. Gong, Y. Li, A. Li and J. Feng, DBP formation and genotoxicity during chlorination of pyrimidines and purines bases, *Chem. Eng. J.*, 2017, **307**, 884–890, DOI: 10.1016/j.cej.2016.09.018.

23 K. Kumar and D. W. Margerum, Kinetics and mechanism of general-acid-assisted oxidation of bromide by hypochlorite and hypochlorous acid, *Inorg. Chem.*, 1987, **26**(17), 2706–2711, DOI: 10.1021/ic00269a039.

24 Y.-H. Chuang, D. L. McCurry, H.-H. Tung and W. A. Mitch, Formation pathways and trade-offs between haloacetamides and haloacetaldehydes during combined chlorination and chloramination of lignin phenols and natural waters, *Environ. Sci. Technol.*, 2015, **49**(24), 14432–14440, DOI: 10.1021/acs.est.5b04783.

25 S. L. Plata, A. E. Childress and D. L. McCurry, Minimizing N-nitrosodimethylamine formation during disinfection of blended seawater and wastewater effluent, *ACS ES&T Water*, 2024, **4**(4), 1498–1507, DOI: 10.1021/acsestwater.3c00617.

26 Z. T. How, I. Kristiana, F. Busetti, K. L. Linge and C. A. Joll, Organic chloramines in chlorine-based disinfected water systems: A critical review, *J. Environ. Sci.*, 2017, **58**, 2–18, DOI: 10.1016/j.jes.2017.05.025.

27 S. Y. Kimura and A. Ortega-Hernandez, Formation mechanisms of disinfection byproducts: Recent developments, *Curr. Opin. Environ. Sci. Health*, 2019, **7**, 61–68, DOI: 10.1016/j.coesh.2018.11.002.

28 B. Prevost, M. Goulet, F. Lucas, M. Joyeux, L. Moulin and S. Wurtzer, Viral persistence in surface and drinking water: Suitability of PCR pre-treatment with intercalating dyes, *Water Res.*, 2016, **91**, 68–76, DOI: 10.1016/j.watres.2015.12.049.

29 A. E. Lobos, A. M. Brandt, J. F. Gallard-Góngora, R. Korde, E. Brodrick and V. J. Harwood, Persistence of sewage-associated genetic markers in advanced and conventional treated recycled water: implications for microbial source tracking in surface waters, *MBio*, 2024, **15**(7), 1–20, DOI: 10.1128/mbio.00655-24.

30 R. J. Bull, *Use of Toxicological and Chemical Models to Prioritize DBP Research*, American Water Works Association, Denver, CO, 2006.

31 Y. Xiang, Z. Deng, X. Yang, C. Shang and X. Zhang, Transformation of adenine and cytosine in chlorination—An ESI-tqMS investigation, *Chemosphere*, 2019, **234**, 505–512, DOI: 10.1016/j.chemosphere.2019.06.116.

32 N. M. Ram and J. Morris, Environmental significance of nitrogenous organic compounds in aquatic sources, *Environ. Int.*, 1980, **4**(5–6), 397–405, DOI: 10.1016/0160-4120(80)90018-5.

33 N. M. Ram, A review of the significance and formation of chlorinated N-organic compounds in water supplies including preliminary studies on the chlorination of alanine, tryptophan, tyrosine, cytosine, and syringic acid, *Environ. Int.*, 1985, **11**(5), 441–451, DOI: 10.1016/0160-4120(85)90227-2.

34 X. Zhang, J. Zhai, Y. Zhong and X. Yang, Degradation and DBP formations from pyrimidines and purines bases during sequential or simultaneous use of UV and chlorine, *Water Res.*, 2019, **165**, 115023, DOI: 10.1016/j.watres.2019.115023.

35 G. Sun, P. Guo, H. Y. Kaw, M. Zhou and W. Wang, Uncovering an emerging group of halogenated nucleobase-derived disinfection byproducts in drinking water: prioritization of the highly cytotoxic 2-chloroadenine, *Environ. Sci. Technol.*, 2023, **57**(23), 8768–8775, DOI: 10.1021/acs.est.3c01484.

36 J. Maity and R. Stromberg, An efficient and facile methodology for bromination of pyrimidine and purine nucleosides with sodium monobromoisocyanurate (SMBI), *Molecules*, 2013, **18**(10), 12740–12750, DOI: 10.3390/molecules181012740.

37 A. Moller, A. Nordheim, S. A. Kozlowski, D. Patel and A. Rich, Bromination stabilizes poly (dG-dC) in the Z-DNA form under low-salt conditions, *Biochemistry*, 1984, **23**(1), 54–62, DOI: 10.1021/bi00296a009.

38 K. H. Rathnayake, M. F. Hossain, A. Brown and S. Y. Kimura, From Micropollutant to DBP Driver: The Unexpected Reactivity of 1-Chlorobenzotriazole in Water Disinfection, *Environ. Sci. Technol.*, 2025, **60**(1), 1218–1228, DOI: 10.1021/acs.est.5c11623.

39 American Public Health Association, R. Baird, A. D. Eaton, E. W. Rice and L. Bridgewater, American Water Works Association and Water Environment Federation, *Standard Methods for the Examination of Water and Wastewater*, American Public Health Association, Washington, DC, 2017, ISBN: 978-0875532998.

40 R. S. Summers, S. M. Hooper, H. M. Shukairy, G. Solarik and D. Owen, Assessing DBP yield: uniform formation conditions, *J. Am. Water Works Assoc.*, 1996, **88**(6), 80–93, DOI: 10.1002/j.1551-8833.1996.tb06573.x.

41 A. Ortega-Hernandez, R. Acayaba, C. Verwold, C. C. Montagner and S. Y. Kimura, Emerging investigator series: emerging disinfection by-product quantification method for wastewater reuse: trace level assessment using tandem mass spectrometry, *Environ. Sci.: Water Res. Technol.*, 2021, **7**(2), 285–297, DOI: 10.1039/D0EW00947D.

42 H. Lei, B. J. Mariñas and R. A. Minear, Bromamine decomposition kinetics in aqueous solutions, *Environ. Sci. Technol.*, 2004, **38**(7), 2111–2119, DOI: 10.1021/es034726h.

43 H. Lei, R. A. Minear and B. J. Mariñas, Cyanogen bromide formation from the reactions of monobromamine and dibromamine with cyanide ion, *Environ. Sci. Technol.*, 2006, **40**(8), 2559–2564, DOI: 10.1021/es0519942.

44 S. Y. Kimura, Y. Komaki, M. J. Plewa and B. J. Mariñas, Chloroacetonitrile and N, 2-dichloroacetamide formation from the reaction of chloroacetaldehyde and monochloramine in water, *Environ. Sci. Technol.*, 2013, **47**(21), 12382–12390, DOI: 10.1021/es4029638.

45 S. Y. Kimura, T. N. Vu, Y. Komaki, M. J. Plewa and B. J. Mariñas, Acetonitrile and N-chloroacetamide formation from the reaction of acetaldehyde and monochloramine, *Environ. Sci. Technol.*, 2015, **49**(16), 9954–9963, DOI: 10.1021/acs.est.5b01875.

46 K. Kumar, R. A. Day and D. W. Margerum, Atom-transfer redox kinetics: general-acid-assisted oxidation of iodide by chloramines and hypochlorite, *Inorg. Chem.*, 1986, **25**(24), 4344–4350, DOI: 10.1021/ic00244a012.

47 K. Huang, K. P. Reber, M. D. Toomey, H. Haflich, J. A. Howarter and A. D. Shah, Reactivity of the polyamide membrane monomer with free chlorine: reaction kinetics, mechanisms, and the role of chloride, *Environ. Sci. Technol.*, 2019, **53**(14), 8167–8176, DOI: 10.1021/acs.est.9b01446.

48 R. P. Dias, M. H. Schammel, K. P. Reber and J. D. Sivey, Applications of 1, 3, 5-trimethoxybenzene as a derivatizing agent for quantifying free chlorine, free bromine, bromamines, and bromide in aqueous systems, *Anal. Methods*, 2019, **11**(43), 5521–5532, DOI: 10.1039/c9ay01443h.

49 S. S. Lau, R. P. Dias, K. R. Martin-Culet, N. A. Race, M. H. Schammel, K. P. Reber, A. L. Roberts and J. D. Sivey, 1, 3, 5-Trimethoxybenzene (TMB) as a new quencher for preserving redox-labile disinfection byproducts and for quantifying free chlorine and free bromine, *Environ. Sci.: Water Res. Technol.*, 2018, **4**(7), 926–941, DOI: 10.1039/c8ew00062j.

50 Y. Pan, X. Zhang, E. D. Wagner, J. Osiol and M. J. Plewa, Boiling of simulated tap water: effect on polar brominated disinfection byproducts, halogen speciation, and cytotoxicity, *Environ. Sci. Technol.*, 2014, **48**(1), 149–156, DOI: 10.1021/es403775v.

51 H. Zhai and X. Zhang, A new method for differentiating adducts of common drinking water DBPs from higher molecular weight DBPs in electrospray ionization-mass spectrometry analysis, *Water Res.*, 2009, **43**(8), 2093–2100, DOI: 10.1016/j.watres.2009.01.013.

52 X. Zhang, J. W. Talley, B. Boggess, G. Ding and D. Birdsell, Fast selective detection of polar brominated disinfection byproducts in drinking water using precursor ion scans, *Environ. Sci. Technol.*, 2008, **42**(17), 6598–6603, DOI: 10.1021/es800855b.

53 P. A. Espinosa-Barrera, M. Gómez-Gómez, J. Vanegas, F. Machuca-Martinez, R. A. Torres-Palma, D. Martínez-Pachón and A. Moncayo-Lasso, Systematic analysis of the scientific-technological production on the use of the UV, H2O2, and/or Cl2 systems in the elimination of bacteria and associated antibiotic resistance genes, *Environ. Sci. Pollut. Res.*, 2024, **31**(5), 6782–6814, DOI: 10.1007/s11356-023-31435-2.

54 M.-F. Pouët, E. Baures, S. Vaillant and O. Thomas, Hidden isosbestic point (s) in ultraviolet spectra, *Appl. Spectrosc.*, 2004, **58**(4), 486–490, DOI: 10.1366/000370204773580365.

55 R. V. Padmanabhuni, J. Luo, Z. Cao and Y. Sun, Preparation and characterization of N-halamine-based antimicrobial fillers, *Ind. Eng. Chem. Res.*, 2012, **51**(14), 5148–5156, DOI: 10.1021/ie300212x.

56 G. Abulikemu, J. H. Mistry, D. G. Wahman, M. T. Alexander, A. R. Kennicutt, J. D. Bollman and J. G. Pressman, Investigation of chloramines, disinfection byproducts, and nitrification in chloraminated drinking water distribution systems, *J. Environ. Eng.*, 2023, **149**(1), 04022070, DOI: 10.1061/(ASCE)EE.1943-7870.0002062.

57 G. J. Kirmeyer, *Optimizing Chloramine Treatment*, American Water Works Association, Denver, 2004, ISBN: 978-1583213193.

58 M. Szabó, F. Simon and I. Fábián, The formation of N-chloramines with proteinogenic amino acids, *Water Res.*, 2019, **165**, 114994, DOI: 10.1016/j.watres.2019.114994.

59 D. W. Margerum, E. T. Gray Jr. and R. P. Huffman, *Chlorination and the Formation of N-Chloro Compounds in Water Treatment*, U.S. Environmental Protection Agency, Cincinnati, 1978, EPA Report No. 600/2-78-172.
60 Q. Shen, T. Zhao, N. J. P. Wawryk, K. N. M. Chau, D. Zhang, K. Carroll, W. Chu, T. Huan and X.-F. Li, Nontargeted analysis of reactive nitrogenous compounds in suwannee river standard reference materials and authentic river water samples, *Environ. Sci. Technol.*, 2024, **58**(35), 15807–15815, DOI: 10.1021/acs.est.4c05165.
61 Z. Hua, J. Li, Z. Zhou, S. Zheng, Y. Zhang and J. Fang, Exploring pathways and mechanisms for dichloroacetonitrile formation from typical amino compounds during UV/chlorine treatment, *Environ. Sci. Technol.*, 2022, **56**(13), 9712–9721, DOI: 10.1021/acs.est.2c01495.
62 C. Shang, W. L. Gong and E. R. Blatchley III, Breakpoint chemistry and volatile byproduct formation resulting from chlorination of model organic-N compounds, *Environ. Sci. Technol.*, 2000, **34**(9), 1721–1728, DOI: 10.1021/es990513+.
63 G. Hua and D. A. Reckhow, Comparison of disinfection byproduct formation from chlorine and alternative disinfectants, *Water Res.*, 2007, **41**(8), 1667–1678, DOI: 10.1016/j.watres.2007.01.032.
64 D. A. Reckhow and P. C. Singer, in *Water Chlorination: Environmental Impact and Health Effects*, ed. R. L. Jolley, K. F. Hoffmann and G. H. Weinberg, CRC Press/Ann Arbor Science, Boca Raton, FL, 1985, vol. 5, pp. 79–118.
65 S. W. Krasner, H. S. Weinberg, S. D. Richardson, S. J. Pastor, R. Chinn, M. J. Sclimenti, G. D. Onstad and A. D. Thruston Jr., Occurrence of a new generation of disinfection byproducts, *Environ. Sci. Technol.*, 2006, **40**(23), 7175–7185, DOI: 10.1021/es060353j.
66 X. Zhang, Z. Chen, J. Shen, S. Zhao, J. Kang, W. Chu, Y. Zhou and B. Wang, Formation and interdependence of disinfection byproducts during chlorination of natural organic matter in a conventional drinking water treatment plant, *Chemosphere*, 2020, **242**, 125227, DOI: 10.1016/j.chemosphere.2019.125227.
67 O. S. Tee, M. J. Kornblatt and C. G. Berks, Mechanisms of bromination of uracil derivatives. 6. Cytosine and N-substituted derivatives, *J. Org. Chem.*, 1982, **47**(6), 1018–1023, DOI: 10.1021/jo00345a025.
68 H. Taguchi and S. Y. Wang, Bromination of cytosine derivatives, *J. Org. Chem.*, 1979, **44**(24), 4385–4393.
69 J. Ao, L. Bu, Y. Wu, Y. Wu and S. Zhou, Enhanced formation of haloacetonitriles during chlorination with bromide: Unveiling the important roles of organic bromamines, *Sci. Total Environ.*, 2023, **868**, 161723, DOI: 10.1016/j.scitotenv.2023.161723.
70 Z. Shen, S. N. Mitra, W. Wu, Y. Chen, Y. Yang, J. Qin and S. L. Hazen, Eosinophil peroxidase catalyzes bromination of free nucleosides and double-stranded DNA, *Biochemistry*, 2001, **40**, 2041–2051.
71 K. S. Pandey and P. C. Mishra, Electronic spectra of 8-bromoguanine and 8-bromoadenine, *J. Photochem. Photobiol., A*, 1991, **62**, 107–115.
72 M. Ikehara, S. Uesugi and M. Kaneko, Bromination of adenine nucleoside and nucleotide, *Chem. Commun.*, 1967, 17–18, DOI: 10.1039/C19670000017.
73 C. Chatgilialoglu, M. Guerra and Q. G. Mulazzani, Model studies of DNA C5 'radicals. Selective generation and reactivity of 2 '-deoxyadenosin-5 '-yl radical, *J. Am. Chem. Soc.*, 2003, **125**, 3839–3848, DOI: 10.1021/ja029374d.
74 H. C. Li, S. D. Yao, Z. H. Zuo, W. F. Wang, J. S. Zhang and N. Y. Lin, Characterization of the reactive intermediates in laser flash photolysis of adenine, adenosine and dAMP using acetone as photosensitizer, *J. Photochem. Photobiol., B*, 1995, **28**, 65–70, DOI: 10.1016/1011-1344(94)07095-6.

